

# Effect of gadolinium ions on the structure and magnetic properties of zinc-borate glasses and glass ceramics

Petru Pascuta · Eugen Culea

Received: 6 June 2011 / Accepted: 13 October 2011 / Published online: 27 October 2011  
© Springer Science+Business Media, LLC 2011

**Abstract** X-ray diffraction (XRD), electron paramagnetic resonance (EPR), and magnetic susceptibility measurements have been employed to investigate the samples from the  $(\text{Gd}_2\text{O}_3)_x \cdot (\text{B}_2\text{O}_3)_{(60-x)} \cdot (\text{ZnO})_{40}$  ( $0 \leq x \leq 20$  mol%) system. The XRD pattern for the prepared samples shows that the vitreous phase is present only for  $x \leq 15$  mol%. For the samples containing 20 mol%  $\text{Gd}_2\text{O}_3$  the presence of a unique crystalline phase,  $\text{GdBO}_3$ , embedded in a vitreous matrix was evidenced. In this case the XRD patterns show the presence of nanometer sized crystals (64 nm) in a glassy matrix. The EPR spectra of the studied samples exhibit three important features with effective  $g$ -values of  $\approx 6$ , 2.8, 2.0 and a weaker feature at  $g \approx 4.8$ . For low  $\text{Gd}_2\text{O}_3$  contents ( $x < 3$  mol%), the EPR spectra have the typical ‘‘U’’-type shape. For higher contents of  $\text{Gd}_2\text{O}_3$  ( $x \geq 3$  mol%), the spectral features are broadened and finally are dominated by a single broad absorption line located at  $g \approx 2.0$ . This broad EPR line is associated to the  $\text{Gd}^{3+}$  ions present predominantly as clustered species. Magnetic susceptibility data show that for  $x > 1$  mol% the  $\text{Gd}^{3+}$  ions are present not only as isolated species but also as species coupled through antiferromagnetic exchange interactions.

## Introduction

In the modern world of technology, vitreous materials play an important role. Among them, glasses containing gadolinium ions have the subject of a great deal of interest

because of their important optical and magnetic properties which recommend them for a wide range of technologically applications in optical communications, laser technology, optical storage devices, and immobilization of radioactive materials [1–9]. These properties are determined by the environment of  $\text{Gd}^{3+}$  ions as well as by the gadolinium content and its distribution in the glass matrix [10]. Whereas the local structure of the  $\text{Gd}^{3+}$  sites seems to be similar in different types of glasses, the correlation between the doping level and clustering depends on the glass type and composition [10]. EPR spectroscopy is one of the most powerful tools that may provide useful information concerning the structural details for the environment of the transition metal and rare earth ions in glasses such as their coordination number and the valence state, local symmetry, and charge compensation as well as the degree of short-range disorder.  $\text{Gd}^{3+}$  ions have been frequently used as paramagnetic probes for exploring the structure and properties of glasses. The EPR signal of the  $\text{Gd}^{3+}$  ( $4f^7$ ,  $^8S_{7/2}$ ) ions located in the host glass matrix, exhibits an X-band EPR spectrum usually consisting of three main features at  $g \approx 6.0$ ,  $g \approx 2.8$ , and  $g \approx 2.0$  [1, 7, 9, 12, 13, 15]. This spectrum is labeled the U spectrum because of its ‘‘ubiquity’’ and  $\text{Gd}^{3+}$  ions are frequently suspected to impose their environment, when present as impurities in glass system [1, 7, 9, 12, 13, 15].

Magnetic susceptibility measurements offered useful information concerning the distribution of gadolinium ions in the host glass matrix and the nature of the magnetic interactions between these ions on various compositional ranges [11–15]. It is well-known that the magnetic interaction between gadolinium ions in glasses consists of superexchange interactions mediated by oxygen ions. The superexchange interactions between the gadolinium

P. Pascuta · E. Culea (✉)  
Department of Physics, Technical University,  
400114 Cluj-Napoca, Romania  
e-mail: eugen.culea@phys.utcluj.ro

ions in oxide glasses were most frequently attributed to antiferromagnetically coupled gadolinium ion pairs [11–13, 15, 16].

Zinc-borate glasses exhibit low melting temperatures, so they are of technological interest owing to their applications in different fields of electronic products [17–19]. This is due to the fact that the higher the polarizability of an ion, the lower the melting temperature of the substance. Low melting glasses, including zinc-borate glasses, have been widely used for lowering the sintering temperature and optimizing coefficient thermal expansion in the field of electric devices such as multi layer ceramic capacitors, low temperature co-fired ceramics (LTCC), plasma display panels, cathode ray tubes, electric modules, etc. [17–19]. In this view, we underline that glasses from the  $\text{Gd}_2\text{O}_3$ – $\text{ZnO}$ – $\text{B}_2\text{O}_3$  system are very valuable potential candidates for LTCC applications [20] since these glasses fulfill one of the essential requirements for LTCC applications, namely that of a low softening temperature. Having in mind these possible application as well as previous structural and magnetic investigations, the  $\text{ZnO}$ – $\text{B}_2\text{O}_3$ -based glasses doped with  $\text{Gd}_2\text{O}_3$  are interesting also from fundamental point of view. In this view it is very important to clarify the role that gadolinium ions are playing in establishing the properties of these glasses and to determine the physical mechanisms which are at the base of these properties.

The purpose of this study was to investigate by XRD, EPR, and magnetic susceptibility measurements the zinc-borate glasses and glass ceramics containing  $\text{Gd}_2\text{O}_3$  in order to obtain information concerning structural and magnetic properties of these samples.

## Experimental

Glasses of the  $(\text{Gd}_2\text{O}_3)_x \cdot (\text{B}_2\text{O}_3)_{(60-x)} \cdot (\text{ZnO})_{40}$  ( $0 \leq x \leq 15$  mol%) system were prepared using  $\text{Gd}_2\text{O}_3$ ,  $\text{H}_3\text{BO}_3$ , and  $\text{ZnO}$  of high purity (99.9%) in suitable proportion. The mechanically homogenized mixtures were melted in sintered corundum crucibles at 1100 °C in an electric furnace. The samples were put into the electric furnace directly at this temperature. After 10 min the molten material was quenched at room temperature by pouring onto a stainless-steel plate.

The XRD measurements were made with a XRD—6000 Shimadzu diffractometer, with a monochromator of graphite for  $\text{Cu-K}\alpha$  radiation ( $\lambda = 1.5406 \text{ \AA}$ ) at room temperature.  $\text{Cu-K}\alpha$  radiation produced at 40 kV and 30 mA scanned the range of diffraction angles ( $2\theta$ ) between  $10^\circ$  and  $60^\circ$  with a  $2\theta$ -step of  $0.02^\circ \text{ s}^{-1}$ .

The EPR measurements were performed using a PS 8400 spectrometer in the X-band (9.1–9.6 GHz) with 100 kHz field modulations. The measurements were made

at room temperature. To avoid the alteration of the glass structure due to the ambient conditions, especially humidity, samples were powdered immediately after preparation and enclosed in tubular holders of the same caliber. Equal quantities of samples were studied.

The magnetic susceptibility measurements were made using a Faraday type magnetic balance in 80–300 K temperature ranges. Corrections due to the diamagnetism of the  $\text{Gd}_2\text{O}_3$ ,  $\text{B}_2\text{O}_3$ , and  $\text{ZnO}$  were taken into account in order to obtain the real magnetic susceptibility of gadolinium ions in the studied samples.

## Results and discussion

### XRD data

The vitreous or/and crystalline nature of the  $(\text{Gd}_2\text{O}_3)_x \cdot (\text{B}_2\text{O}_3)_{(60-x)} \cdot (\text{ZnO})_{40}$  system with various contents of gadolinium oxide ( $0 \leq x \leq 20$  mol%) was tested by XRD. For samples with  $x \leq 15$  mol% the XRD patterns exhibit a broad diffuse scattering at low angles confirming a long-range structural disorder characteristic of vitreous network [21]. For the sample with the 20 mol%  $\text{Gd}_2\text{O}_3$  content the vitreous phase coexists with a crystalline phase and the pattern shows a large maximum overlapped with the peaks characteristic to the crystalline phase (Fig. 1).

All detectable peaks can be indexed as belonging to the  $\text{GdBO}_3$  crystal in the standard data (PDF#130483).  $\text{GdBO}_3$  crystallizes in hexagonal system with the following lattice

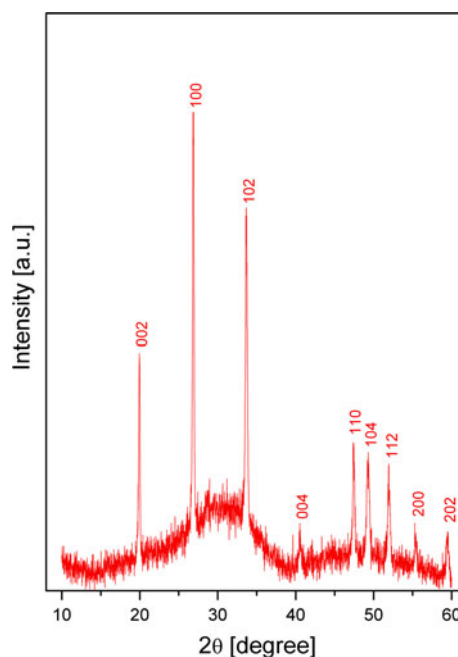


**Fig. 1** The XRD patterns of sample with 20 mol%  $\text{Gd}_2\text{O}_3$

parameters:  $a = 3.84 \text{ \AA}$  and  $c = 8.905 \text{ \AA}$  very close to those of the standard data PDF#130483 ( $a = 3.829 \text{ \AA}$  and  $b = 8.89 \text{ \AA}$ ). Owing to their high vacuum ultraviolet transparency, good vacuum ultraviolet absorption, and exceptional optical damage threshold in the vacuum ultraviolet range, rare earth orthoborates ( $\text{RBO}_3$ ,  $\text{R} = \text{Gd}$  and  $\text{Y}$ ) with the hexagonal varied-type structure are an interesting class of materials [22, 23]. For the sample with 20 mol%  $\text{Gd}_2\text{O}_3$ , from the full width at half maximum for all peaks of the refined diffraction line profiles, the average crystallite size of the crystalline phase has been determined by using the Debye–Scherrer formula [24]:

$$D = \frac{\lambda \cdot K}{\beta \cdot \cos\theta} \tag{1}$$

where  $D$  is the apparent volume-weighted crystallite size,  $\lambda$  is the X-rays wavelength ( $1.54060 \text{ \AA}$ , in this case),  $K = 0.89$  (the Scherrer constant),  $\beta$  is the width of line at the half-maximum intensity in radians and  $\theta$  is the Bragg angle. From Debye–Scherrer calculation, the average crystallite size of the sample with 20 mol%  $\text{Gd}_2\text{O}_3$  is 64 nm, so it lies in the nanometer range.

EPR data

The EPR spectra at room temperature obtained for samples from the  $(\text{Gd}_2\text{O}_3)_x \cdot (\text{B}_2\text{O}_3)_{(60-x)} \cdot (\text{ZnO})_{40}$  system with  $0.5 \leq x \leq 20$  mol%, are shown in Fig. 2. As it is well-known, the EPR spectra are sensitive to the local symmetry of the involved paramagnetic ions giving information about their valence states and interactions. As can be seen from Fig. 2, there is a strong dependence of the EPR spectra and the  $\text{Gd}_2\text{O}_3$  content of the samples. In the case of  $\text{Gd}^{3+}$  the experimental EPR resonance absorption can be analyzed using a spin Hamiltonian which incorporates the Zeeman and the crystal-field (CF) interactions [25–28]:

$$H = H_{\text{Zeeman}} + H_{\text{CF}} \tag{2}$$

For  $\text{Gd}^{3+}$  ions which belong to the  $4f^7$  configuration with  $^8\text{S}_{7/2}$  as ground state in the free ion the Zeeman interaction term (for  $L = 0$ ) can be written as:

$$H_{\text{Zeeman}} = g_0 \beta B S \tag{3}$$

where  $g_0 = 2.00$ ,  $\beta$  is the Bohr magnetron,  $B$  is the applied magnetic field,  $S = 7/2$  is the spin angular momentum, and  $L$  is the orbital angular momentum. The term due to the CF interactions can be written in terms of spin operators  $O_k^q$  as defined by Abragam and Bleaney [29]:

$$H_{\text{CF}} = \sum_{k,q} b_k^q O_k^q \tag{4}$$

where the spin operators  $O_k^q$  have their corresponding CF parameters  $b_k^q$ . The number of  $(k, q)$  combinations depends

on the symmetry of the CF around the  $\text{Gd}^{3+}$  ions, and  $k = 2, 4, 6$  and  $0 \leq q \leq k$ . To explain the U-spectrum of  $\text{Gd}^{3+}$  ions is sufficient to restrict the Hamiltonian to terms of second degree in the spin operators and higher order of CF terms could be neglected [25–28]:

$$H = g_0 \beta B S + \frac{1}{3} (b_2^0 O_2^0 + b_2^2 O_2^2) \tag{5}$$

There are two important extremes when perturbation theory approaches may be used [25, 26]: (i) the strong-field Zeeman effect or weak CF limit,  $H_{\text{Zeeman}} \gg H_{\text{CF}}$ ; and (ii) the weak-field Zeeman effect or strong CF limit,  $H_{\text{CF}} \gg H_{\text{Zeeman}}$ . If all the gadolinium ions in a sample are in the weak CF limit, the EPR spectrum consists of resonances centered in the vicinity of  $g \approx 2.0$ . This case is common for  $\text{Gd}^{3+}$  ions in cubic crystals. The second case is expected only when the local symmetries of the  $\text{Gd}^{3+}$  ions depart substantially from cubic symmetry. In this case the EPR spectrum consists of the few resonances resulting from transitions within the widely separated Kramers levels. Since the ions are randomly oriented these are the  $g$  values that are turning values with respect to orientation or are at least relatively constant over an appreciable range of field directions. They occur mainly in the range where  $g > 2$ . Brodbeck and Iton [26] concluded that the U-spectrum of  $\text{Gd}^{3+}$  ions could be interpreted only with a broad distribution of values for  $b_2^0$  and with a distribution of values of  $b_2^2$  such that the ratio  $\lambda = b_2^2/b_2^0$  has an appreciable probability over the whole range  $0 < \lambda < 1$ . The resonance absorptions from  $g \approx 6.0$  and  $g \approx 2.8$  are identified with specific EPR transitions that are stationary with respect to  $b_2^2$  and  $\lambda$ , and the orientation angles of the applied field  $B$  over a wide range. The magnitude of the CF interactions in glasses is indicative of a moderate distortion of a cubic, octahedral or tetrahedral CF, and is expected to occur when the gadolinium ions are able to achieve a high coordination number ( $\geq 6$ ) within the structurally disordered matrices. In this case the  $\text{Gd}^{3+}$  ions will play a network modifier role in glasses that is usual for the rare-earth ions [26]. Thus, the site symmetries of the gadolinium ions in glasses are essentially low and disordered, which dictate their own environments in glasses and are best characterized by a single low symmetry type sites as proposed by Griscom [30].

In this study, for low content of gadolinium ions content ( $x \leq 1$  mol%) the EPR spectra show well-known features with  $g \approx 6.0$ ;  $\approx 2.8$ , and  $\approx 2.0$  characteristic of the so-called ‘‘U’’ spectrum which are typical for  $\text{Gd}^{3+}$  ions uniformly distributed in the glass matrix. They are associated with  $\text{Gd}^{3+}$  ions located at sites with weak crystalline fields of different symmetries (tetrahedral, octahedral, and cubic with moderate distortions) having coordination numbers higher than six [1, 7, 12, 13, 15, 31]. The most important difference

between the EPR spectra of  $\text{Gd}^{3+}$  ions from our samples and the “U” spectrum consists in the appearance of an asymmetric absorption line at  $g \approx 4.8$  (Fig. 2). The presence of this resonance absorption line suggests that in studied samples some  $\text{Gd}^{3+}$  ions are also located at sites with relatively strong CF having an orthorhombic symmetry and a coordination number lower than six. This location for  $\text{Gd}^{3+}$  ions is unusual being known the general tendency of rare-earth ions associated with high coordination numbers [1, 7, 12, 13, 15, 31]. In principle, these sites may be of network glass former or network glass modifier type. Ionic radius considerations suggest that  $\text{Gd}^{3+}$  ions ( $r_{\text{Gd}^{3+}} \approx 0.94 \text{ \AA}$ ) cannot substitute the much smaller boron ions ( $r_{\text{B}} \approx 0.23 \text{ \AA}$ ). In this case the  $\text{Gd}^{3+}$  ions will play a network glass modifier role in the studied samples. The increasing of the gadolinium ions content in studied samples leads to EPR line broadening of both sites of  $\text{Gd}^{3+}$  ions. This broadening is naturally ascribed to dipole–dipole interactions between the  $\text{Gd}^{3+}$  ions with the increase of  $\text{Gd}_2\text{O}_3$  content or/and to the increase of disordering in the glass structure. The EPR line shape is also influenced by the structure of the zinc-borate glasses in which the gadolinium ions are incorporated. The environment of  $\text{Gd}^{3+}$  ions is determined by a competition between structural characteristics of the zinc-borate glasses and the local structure appropriate for  $\text{Gd}^{3+}$  ions. The FTIR data of the studied samples [21] shows that at low contents of gadolinium ions the replace of  $\text{B}_2\text{O}_3$  with  $\text{Gd}_2\text{O}_3$  leads to the increase of the number of  $\text{BO}_4$  structural units, while for higher  $\text{Gd}_2\text{O}_3$  contents, the  $\text{BO}_4$  structural units will be destroyed and converted into  $\text{BO}_3$  and  $\text{BO}_2\text{O}^-$  structural

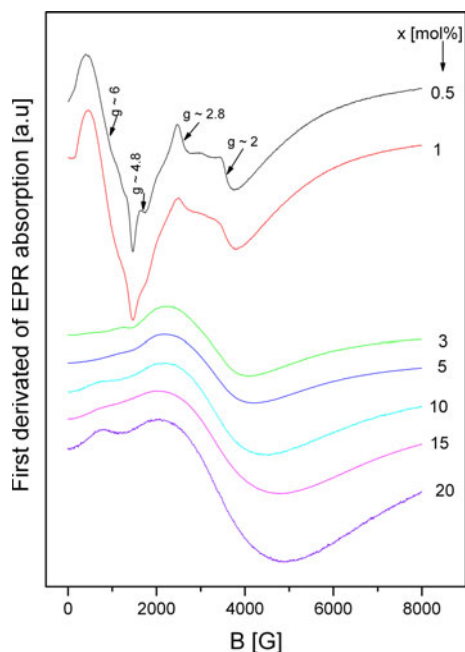


**Fig. 2** EPR spectra of  $\text{Gd}^{3+}$  ions in the  $(\text{Gd}_2\text{O}_3)_x \cdot (\text{B}_2\text{O}_3)_{(60-x)} \cdot (\text{ZnO})_{40}$  samples

units with non-bridging oxygens (NBO). Thus, the gradual increasing of the  $\text{Gd}_2\text{O}_3$  content in the glasses leads to the progressive formation of NBOs which destroys the local ordering of the  $\text{Gd}^{3+}$  ion vicinities and changes the coordination of  $\text{Gd}^{3+}$  ions. So for higher  $\text{Gd}_2\text{O}_3$  content the EPR spectra become less resolved and they are dominated by a single broad absorption line located at  $g \approx 2.0$  associated to  $\text{Gd}^{3+}$  ions present predominantly as clustered species [7, 13, 15, 30]. For samples with  $x \geq 3 \text{ mol\%}$  the evolution of this resonance line with increasing the gadolinium ions content was followed in dependence of the EPR parameters, i.e., the line intensity ( $J$ ) and the linewidth ( $\Delta B$ ). The corresponding variations of these parameters are plotted in Fig. 3. The line intensity and linewidth of the  $g \approx 2.0$  absorption line increase as function of  $x$ . In general, the signal intensity is proportional to the number of EPR active species involved in the resonance absorption, so the increase of the line intensity indicates an increase in  $\text{Gd}^{3+}$  ion concentration. The  $\Delta B = f(x)$  dependence reflects the competition between the broadening mechanisms (due to the dipole–dipole interactions and the increased disordering of the matrix structure) and the narrowing ones (due to the superexchange interactions within the pairs of gadolinium ions). These mechanisms act simultaneously but one of them may become predominant in function of the  $\text{Gd}_2\text{O}_3$  content of the samples. The evolution of the line intensity and linewidth of the resonance absorption from  $g \approx 2.0$  with the increasing of the  $\text{Gd}_2\text{O}_3$  content shows a gradual increase of the number of superexchange coupled Gd–O–Gd pairs in the studied samples.

### Magnetic susceptibility data

The magnetic susceptibility data correlate well with the EPR results and also complete them. The temperature

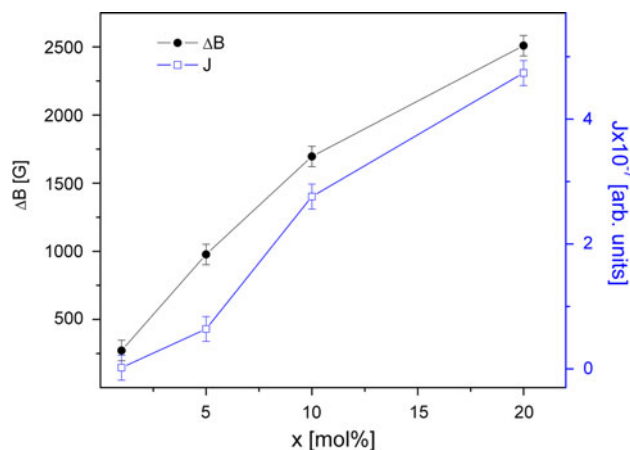


**Fig. 3** Composition dependence of line intensity and linewidth for  $g \approx 2.0$  absorption line of  $(\text{Gd}_2\text{O}_3)_x \cdot (\text{B}_2\text{O}_3)_{(60-x)} \cdot (\text{ZnO})_{40}$  samples. The lines are drawn as a guide for the eyes

dependence of the reciprocal magnetic susceptibility of studied samples is presented in Fig. 4. For the sample with  $x = 1$  mol% a Curie type behavior is observed which is typical for isolated gadolinium ions or/and subjected to dipole–dipole interactions. For  $x > 1$  mol% the reciprocal magnetic susceptibility follows the Curie–Weiss law:

$$\chi = \chi_0 + \frac{C_M}{T - \theta_p} \tag{6}$$

and

$$C_M = \frac{\mu_{\text{eff}}^2 \cdot N_A}{3k_B} x \tag{7}$$

where  $\chi_0$  is the temperature-independent contribution,  $C_M$  is the molar Curie constant,  $T$  is the absolute temperature in Kelvins,  $\theta_p$  is the paramagnetic Curie temperature,  $\mu_{\text{eff}}$  is the effective magnetic moment,  $N_A$  is the Avogadro’s number,

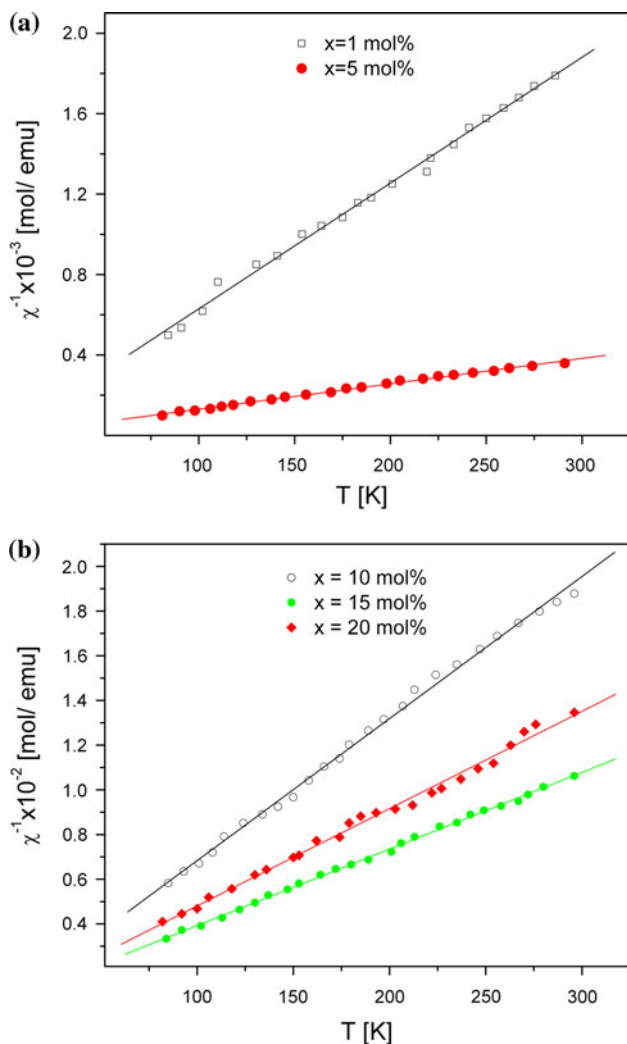


**Fig. 4** Temperature dependence of the reciprocal magnetic susceptibility for  $(\text{Gd}_2\text{O}_3)_x(\text{B}_2\text{O}_3)_{(60-x)}(\text{ZnO})_{40}$  samples with  $1 \leq x \leq 5$  mol % (a) and with  $10 \leq x \leq 20$  mol% (b)

$x$  is the concentration of gadolinium ions in the sample and  $k_B$  is the Boltzmann’s constant. This suggests that in the samples with  $x > 1$  mol% the  $\text{Gd}^{3+}$  ions are present as both isolated and coupled species. The small and negative values of  $\theta_p$  (Fig. 5) obtained for the samples with  $x > 1$  mol% suggest the presence of weak antiferromagnetic interactions between the gadolinium ions located in the vitreous host glass matrix. The  $\theta_p$  is a rough indicator of both the strength of the interaction between the magnetic moments and the number of magnetic ions participating in the interactions. The absolute magnitude of  $\theta_p$  values increases with increasing the  $\text{Gd}_2\text{O}_3$  content,  $x$ , suggesting that the magnetic interactions become stronger at higher  $x$  values (Fig. 5). By using the molecular field model [32], the molecular field constant is given by:

$$J = \left| \frac{\theta_p}{C_M} \right| = 2z \frac{J_{ij}}{Ng^2\mu_B^2}, \tag{8}$$

where  $C_M$  is the molar Curie constant,  $N$  and  $z$  are the total and the exchange coupled number of magnetic ions,  $g$  is their spectroscopic splitting factor,  $J_{ij}$  is the magnetic exchange integral and  $\mu_B$  is the Bohr magneton. The values of molecular field constant, obtained from experimental data, are plotted in Fig. 5. For  $x = 1$  mol% we have  $J = 0$  while for  $x \geq 5$  mol% the absolute values of  $J$  is approximately constant with increasing the gadolinium ions content. This behavior shows that the  $z/N$  ratio is constant, the number of superexchange coupled  $\text{Gd}^{3+}$  ions being proportional to the total number of magnetic ions in the studied samples as expected for a system with random distribution of gadolinium ions. The values of the effective magnetic moment (in Bohr magneton) of gadolinium ions in the studied samples can be calculated from the experimentally determined values of the molar Curie constant as follows [7, 13, 15, 16, 33]:

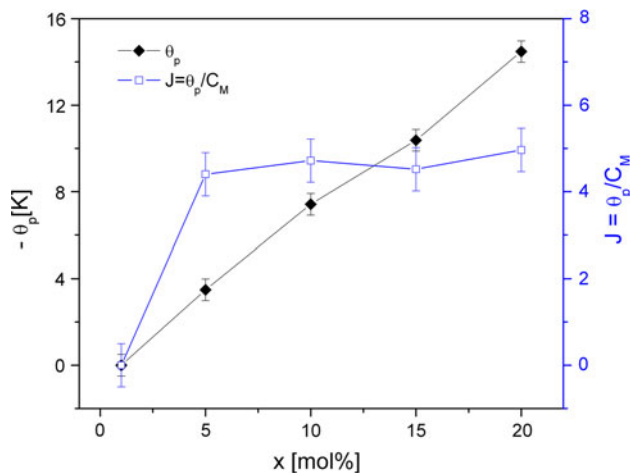


**Fig. 5** The composition dependence of the paramagnetic Curie temperature and molecular field constant for  $(\text{Gd}_2\text{O}_3)_x(\text{B}_2\text{O}_3)_{(60-x)}(\text{ZnO})_{40}$  samples. The solid line is only a guide for the eye

**Table 1** Molar Curie constants and experimental values of  $\mu_{\text{eff}}$  for the  $(\text{Gd}_2\text{O}_3)_x(\text{B}_2\text{O}_3)_{(60-x)}(\text{ZnO})_{40}$  samples

$x$ [mol% $\text{Gd}_2\text{O}_3$ ]	$C_M (\pm 5 \times 10^{-4} \text{ emu/mol})$	$\mu_{\text{eff}} (\pm 1 \times 10^{-2} \mu_B)$
1	0.15983	7.99
5	0.79261	7.95
10	1.57269	7.93
15	2.29721	7.82
20	2.91706	7.63

$$\mu_{\text{eff}} = \sqrt{\frac{3k_B}{N_A \mu_B^2}} \cdot \sqrt{\frac{C_M}{2x}} = 2.827 \sqrt{\frac{C_M}{2x}} \quad (9)$$

The values obtained for  $\mu_{\text{eff}}$  and  $C_M$  are given in Table 1. The experimental values of  $\mu_{\text{eff}}$  were found to be very close to that for the magnetic moment of  $\text{Gd}^{3+}$  ions in free ion state,  $\mu_{\text{Gd}^{3+}} = 7.98 \mu_B$  [34], indicating in the case of the  $x \leq 1$  mol% samples and somewhat smaller for the  $x > 1$  mol% ones. The values of  $\mu_{\text{eff}}$  obtained for the  $\text{Gd}^{3+}$  ions in these glasses as well as their evolution with respect to  $x$  support the assumption of the presence of weak antiferromagnetic interaction between the gadolinium ions in the samples with  $x > 1$  mol%. Aggregates of Gd–O–Gd coupled pairs lead to the appearance of magnetic clusters each having an effective magnetic moment. The values obtained from magnetic susceptibility measurements are average values. In the studied samples some gadolinium ions behave as free  $\text{Gd}^{3+}$  ions, while others occur as antiferromagnetically coupled pairs with a certain angle between the magnetic moments. Close to 0 K this angle is  $180^\circ$  and becomes, on an average, smaller at higher temperatures so that magnetic moments corresponding to coupled pairs are lower than for uncoupled ions. The proportion of isolated species/antiferromagnetically coupled species  $\text{Gd}^{3+}$  depends on the structure of the zinc borate glasses. The increase of the number of NBOs as a function of  $\text{Gd}_2\text{O}_3$  content in these samples leads to the decrease of glass polymerization which can be correlated with the increase of the superexchange interactions between  $\text{Gd}^{3+}$  ions. The magnetic susceptibility data obtained for zinc borate glasses and glass ceramics doped with gadolinium ions are in agreement with those previously reported for other glasses and glass ceramics containing  $\text{Gd}_2\text{O}_3$  [7, 12, 13, 15, 16, 29, 35] and support the EPR results presented in this study.

## Conclusions

Homogeneous glasses of the  $(\text{Gd}_2\text{O}_3)_x(\text{B}_2\text{O}_3)_{(60-x)}(\text{ZnO})_{40}$  system were obtained within the  $0 \leq x \leq 15$  mol% composition range while the sample with 20 mol%  $\text{Gd}_2\text{O}_3$  was a

glass ceramic. The crystalline phase of the glass ceramic sample was identified to be the  $\text{GdBO}_3$  which crystallizes in hexagonal system. The crystallite size of the gadolinium borate is 56 nm, so it lies in the nano-range. The EPR spectra of the studied samples reveal, in addition to the “U” pattern, typical of  $\text{Gd}^{3+}$  ions in glasses, a resonance absorption line centered at  $g \approx 4.8$  assigned to low coordinated  $\text{Gd}^{3+}$  ions disposed in sites with high CF. Another part of  $\text{Gd}^{3+}$  ions will impose a preferential environment, with a relatively weak CF like in other glass matrices and will give rise to the “U” spectrum. Magnetic susceptibility and EPR data evidence that for low  $\text{Gd}_2\text{O}_3$  content ( $x \leq 1$  mol%), the  $\text{Gd}^{3+}$  ions appear as isolated species randomly distributed in the host glass matrix. For higher content of gadolinium ions the temperature dependence of magnetic susceptibility follows the Curie–Weiss law with a small value of  $\theta_p$  indicating the presence of weak antiferromagnetic superexchange interaction between the gadolinium ions in the studied samples. For the samples with  $x > 1$  mol% the  $\mu_{\text{eff}}$  of  $\text{Gd}^{3+}$  ions are lower than the value for free ion. This result is explained by assuming the formation of Gd–O–Gd coupled pairs in which the ions are coupled by superexchange interactions.

**Acknowledgement** This study was supported by CNCSIS—UEFI-SCSU, project number PNII—IDEI 226/2008.

## References

- Malchukova E, Boizot B, Ghaleb D, Petite G (2006) *J Non Cryst Solids* 352:297
- Pascuta P, Culea E (2008) *Mater Lett* 62:4127
- Pascuta P, Borodi G, Culea E (2008) *J Non Cryst Solids* 354:5475
- Xu Z, Chen Y, Lin Y, Gong X, Luo Z, Huang Y (2009) *J Alloys Compd* 481:411
- Pascuta P, Borodi G, Culea E (2009) *J Mater Sci Mater Electron* 20:360
- Koepke C, Piatkowski D, Wisniewski K, Naftaly M (2010) *J Non Cryst Solids* 356:435
- Pascuta P (2010) *J Mater Sci Mater Electron* 21:338
- Paulose PI, Jose G, Unnikrishnan NV (2010) *J Non Cryst Solids* 356:93
- Rada S, Culea E, Rada M (2010) *J Non Cryst Solids* 356:1277
- Kliva J, Edelman IS, Potseluyko AM, Petrakovskaja EA, Berger R, Bruckental I, Yeshurun Y, Malakhovskii AV, Zarubina TV (2003) *J Phys Condens Mater* 15:6671
- Valente MA, Mendiratta SK (1992) *Phys Chem Glasses* 33:149
- Simon S, Pop R, Simon V, Coldea M (2003) *J Non Cryst Solids* 331:1
- Culea E, Pop L, Simon S (2004) *Mater Sci Eng B* 112:59
- Kliva J, Edelman IS, Potseluyko AM, Petrakovskaja EA, Berger R, Bruckental I, Yeshurun Y, Malakhovskii AV, Zarubina TV (2004) *J Mag Mag Mater* 272–276:e1647
- Pascuta P, Bosca M, Culea M, Simon S, Culea E (2008) *Mod Phys Lett B* 22:447
- Saddeek YB, Yahia IS, Aly KA, Dobrowolski W (2010) *Solid State Sci* 12:1426
- Lu SG, Kwok KW, Chan HLW, Choy CL (2003) *Mater Sci Eng B* 99:491

18. Raju GN, Reddy MS, Sudhakar KSV, Veeraiah N (2007) *Opt Mater* 29:1467
19. Zhou L, Lin H, Chen W, Lua L (2008) *J Phys Chem Solids* 69:2499
20. Jo YH, Yeon DH, Mohanty BC, Cho YS (2008) *Met Mater Int* 14:493
21. Pascuta P, Culea E (2011) *J Mater Sci Mater Electron* 22:1060
22. Zhang ZY, Zhang YH, Li XL, Xu JH, Huang Y (2008) *J Alloys Compd* 455:280
23. Yang Z, Wen Y, Sun N, Wang Y, Huang Y, Gao Z, Tao Y (2010) *J Alloys Compd* 489:L9
24. Scherrer P (1918) *Math Physik Klasse* 2:98
25. Iton LE, Brodbeck CM, Suib SL, Stucky GD (1983) *J Chem Phys* 79:1185
26. Brodbeck CM, Iton LE (1985) *J Chem Phys* 83:4285
27. Furniss D, Harrist EA, Hollis DB (1987) *J Phys C Solid State Phys* 20:L147
28. Legeint C, Buzare YJ, Silly G, Jacoboni C (1996) *J Phys Condens Matter* 8:4339
29. Abragam A, Bleaney B (1970) *Electron paramagnetic resonance of transition ions*. Clarendon, Oxford
30. Griscom DL (1980) *J Non Cryst Solids* 40:211
31. Simon S, Ardelean I, Filip S, Bratu I, Cosma I (2000) *Solid State Commun* 116:83
32. Bates LF (1961) *Modern magnetism*. Cambridge University Press, London
33. Ardelean I, Gliguta L (2007) *J Non Cryst Solids* 353:2363
34. Ardelean I, Burzo E, Mitulescu-Ungur D, Simon S (1992) *J Non Cryst Solids* 146:256
35. Simon S, Udvar AD (2010) *J Am Ceram Soc* 93:2760